Published in final edited form as:
J Comp Neurol. 2010 May 15; 518(10): 1862–1878. doi:10.1002/cne.22308.

Projections of PreBötzinger Complex Neurons in Adult Rats

Wenbin Tan, **Silvia Pagliardini**, **Paul Yang**, **Wiktor A. Janczewski**, and **Jack L. Feldman***
Department of Neurobiology, David Geffen School of Medicine at UCLA, Los Angeles, California 90095

Abstract

The preBötzinger Complex (preBötC) contains neural microcircuitry essential for normal respiratory rhythm generation in rodents. A subpopulation of preBötC neurons expresses somatostatin, a neuropeptide with a modulatory action on breathing. Acute silencing of a subpopulation of preBötC neurons transfected by a virus driving protein expression under the somatostatin promoter results in persistent apnea in awake adult rats. Given the profound effect of silencing these neurons, their projections are of interest. We used an adeno-associated virus to overexpress enhanced green fluorescent protein driven by the somatostatin promoter in preBötC neurons to label their axons and terminal fields. These neurons send brainstem projections to: 1) contralateral preBötC; 2) ipsi- and contralateral Bötzinger Complex; 3) ventral respiratory column caudal to preBötC; 4) parafacial respiratory group / retrotrapezoid nucleus; 5) parahypoglossal nucleus/nucleus of the solitary tract; 6) parabrachial/Kölliker-Fuse nuclei; and 7) periaqueductal gray. We did not find major projections to either cerebellum or spinal cord. We conclude that there are widespread projections from preBötC somatostatin-expressing neurons specifically targeted to brainstem regions implicated in control of breathing, and provide a network basis for the profound effects and the essential role of the preBötC in breathing.

INDEXING TERMS

preBötzinger Complex; breathing; respiratory rhythm; AAV2

Breathing is a continuously regulated and essential behavior in vertebrates. The preBötzinger Complex (preBötC) (Smith et al., 1991) in the ventrolateral medulla contains neural microcircuitry essential for respiratory rhythm generation in rodents (Feldman and Del Negro, 2006; Tan et al., 2008). The preBötC is necessary and sufficient to generate a respiratory-related rhythm in neonatal rodent medullary slice preparations in vitro (Smith et al., 1991; Gray et al., 1999), and contains a necessary neuronal network for maintaining normal respiratory activity in rodents in vivo (Gray et al., 2001; Janczewski and Feldman, 2006; Tan et al., 2008). A subpopulation of preBötC neurons that expresses the neurokinin-1 receptor (NK1R) defines its location (Gray et al., 1999). Ablation of ≈80% of preBötC NK1R neurons by saporin-conjugated substance P (SAP-SP) in adult rats causes repeated apneas, initially during REM sleep and progressively during non-REM sleep and wakefulness (Gray et al., 2001; McKay et al., 2005). The neuropeptide somatostatin (Sst) is expressed in a partially overlapping neuronal population in this area, providing an additional

*CORRESPONDENCE TO: J.L.Feldman, Department of Neurobiology, David Geffen School of Medicine at UCLA, Los Angeles, CA 90095-1763. feldman@ucla.edu.
The first two authors contributed equally to this work.

Additional Supporting Information may be found in the online version of this article.

anatomical marker for the preBötC (Pagliardini et al., 2003; Stornetta et al., 2003; Tan et al., 2008).

In order to further test the functional role of the preBötC in breathing, we overexpressed the *Drosophila* allatostatin receptor (AlstR) and enhanced green fluorescent protein (EGFP) by injecting into the preBötC a virus driving AlstR expression with the Sst promoter. The transfection efficiency was about ≈500 neurons on each side. In awake adult rats, activation of AlstRs by exogenous application of allatostatin silenced these neurons, producing within minutes a persistent apnea that would result in asphyxiation (Tan et al., 2008). This is the only known instance where silencing a population of ≈1,000 neurons can completely stop breathing in awake adult mammals.

Understanding the role of the neurons transfected by preBötC injections of a virus expressing AlstR driven by the Sst promoter requires determination of their projections, particularly to other regions known to affect breathing. Here, we systematically mapped these projections. We produced an adeno-associated virus 2 (AAV2) that labels neurons by using the Sst promoter to drive the expression of EGFP cDNA (Tan et al., 2008). When EGFP is expressed in a neuron, it diffuses to fill it in its entirety, including its axon and terminal field. This allowed us to specifically identify and target the projections of this subpopulation of preBötC neurons throughout the nervous system. We identified strong projections to brainstem areas implicated in control of breathing: 1) contralateral preBötC; 2) ipsi- and contralateral Bötzinger Complex (BötC); 3) ventral respiratory group (VRG), caudal to preBötC; 4) parafacial respiratory group / retrotrapezoid nucleus (pFRG/RTN); 5) parahypoglossal nucleus/nucleus of the solitary tract (NTS); 6) parabrachial/Kölliker-Fuse nuclei (PB/KF); and 7) periaqueductal gray (PAG). These extensive projections provide a network basis for the profound role we hypothesize for these neurons in generation of respiratory rhythm.

MATERIALS AND METHODS

Adeno-associated viral vector construction and AAV2 preparation

AAV with an expression cassette of the somatostatin promoter driving EGFP, flanked by the AAV inverted terminal repeats (ITRs), was described previously (Tan et al., 2008). Briefly, the mouse Sst promoter (2.0 kb, ≈81% homology with rat Sst promoter) was amplified by the primers (5′ TTC GAA AGC CTA GAG GCA GAG CAA GCG CTG 3′ and 5′ ACA TGT C GCT ATG GAG CTC TCC ACG GTC TCC 3′; the underlines indicate the BstBI and PciI sites, respectively) from BAC RP23-274H19 and cloned into TOPO-T vector (Invitrogen, Carlsbad, CA). The Sst promoter fragment was cleaved by BstBI and PciI and inserted into BstBI with NcoI sites of pA-Syn-AlstR-IRES-EGFP (Tan et al., 2006) to construct the pA-SST-EGFP. The constructs were verified by sequencing.

AAV2 was prepared using AAV Helper-Free System (Stratagene, La Jolla, CA) according to the manufacturer's instructions. In brief, AAV-293 cells in 150-mm dishes were transfected with 16 μg each of pAAV-RC, pHelper, and a cloning viral vector generated above by using lipofectamine (Invitrogen, Carlsbad, CA) to produce AAV2. The cells were harvested at 72 hours post-transfection, lysed in 15 mL of gradient buffer (10 mM Tris, pH 7.6, 150 mM NaCl, 10 mM $MgCl_2$) by four freeze/thaw cycles in dry ice/ethanol and 37°C bath, with addition of passing through a syringe with a 23G needle 10 times. The lysate was treated by 50 U/mL of benzonase (Sigma, St. Louis, MO) for 30 minute at 37°C and clarified by centrifuge at 3,000*g* for 15 minutes. The virus was purified by using iodixanol density gradient ultracentrifuge at 350,000*g* for 1 hour at 18°C as described elsewhere (Zolotukhin et al., 1999). The AAV2 was further concentrated using 50 kD cutoff

concentrator. The AAV2 was stored at 4°C until use. The titer of the AAV2 was determined by quantitative polymerase chain reaction (PCR) using two EGFP primers.

Surgical procedures

All experimental procedures were approved by the Chancellor's Animal Research Committee at the University of California, Los Angeles. The surgical procedures were described previously (Gray et al., 2001; McKay et al., 2005; Tan et al., 2008). Briefly, male Sprague–Dawley rats (220 – 250 g) were anesthetized with ketamine (100 mg kg^{-1}) and xylazine (10 mg kg^{-1}) injected intraperitoneally (i.p.). During the surgery the rats breathed 1–1.5 vol% isoflurane in oxygen. The rats were positioned in a stereotaxic apparatus with bregma 5 mm below lambda. The dorsal surface of the medulla was exposed. Using a micropipette (40 μm tip diameter) guided by a micromanipulator, AAV2 virus (0.5 μL of 10^9 particles mL^{-1}) in phosphate-buffered saline (PBS, pH 7.2) was injected into left and right preBötC at coordinates: 0.9 mm rostral, ±2 mm lateral and 2.8 mm ventral to the calamus scriptorius. We and many others have established that these coordinates represent the center of the preBötC in adult rats as defined by the distance from bregma, the relative location to the nucleus ambiguus, the inferior olive, and the distance from the facial nucleus (Wang et al., 2001; Gray et al., 2001; Guyenet et al., 2002; Monnier et al., 2003; McKay et al., 2005). Microinjections were made at the rate of 0.2 μL min^{-1} using a series of pressure pulses (PicoSpritzer III, Parker Hannifin, Cleveland, OH). The micropipette was left in place for 5 minutes postinjection to allow the viral solution to be absorbed and to minimize the backflow of the solution up to the micropipette track. After surgery, the rats were housed for 4 – 12 weeks to allow expression of EGFP.

Antibody characterization and immunohistochemistry

The summary of primary antibodies used in the study is shown in Table 1. Primary antibodies used in this study were the following: anti-neurokinin 1 receptor (NK1R) (Advanced Targeting Systems, San Diego, CA; #AB-N04; 1:1,000 dilution) was raised in rabbit using a synthetic peptide corresponding to the 393– 407 amino acid sequence of NK1R. The antiserum recognizes the NK1R in rat, mouse, and guinea pig (technical information provided by Advanced Targeting Systems). The specificity of the antibody has been previously demonstrated (Vigna et al., 1994): the antibody exclusively labeled rat kidney epithelial cells, neurons in the dorsal horn of the spinal cord in the regions corresponding to SP inputs (substantia gelatinosa), as well as neurons and muscle cells in the ileum; Western blot analysis of proteins obtained from rat kidney epithelial cells that expressed functional NK1Rs showed a broad immunoreactive band corresponding to the NK1R (70 to over 150 kDa). The specificity of the antibody has been further confirmed by demonstrating that it exclusively colabels neurons that have internalized fluorescent SP and thus express the NK1R (Pagliardini et al., 2005). Labeling using this antibody was abolished following preadsorption of diluted antiserum with the immunogenic amino acid sequence (NK1R393-407) (Vigna et al., 1994) and by lack of staining in tissue in which neurons expressing the NK1R were killed using saporin-conjugated SP (Mantyh et al., 1997).

Anti-somatostatin (Sst) antibody (Peninsula Laboratories, LLC/Bachem, Torrance, CA; #T-4103, dilution 1:500 or 1:5,000 for Tyramide System Amplification, TSA, see below) was raised in rabbit and was prepared against the first 14 aa of the synthetic peptide Sst. The antibody is specific for Sst; no crossreactivity of the antibody with other peptides such as SP, amylin, glucagon, insulin, neuropeptide Y (NPY), and vasoactive intestinal peptide has been reported according to the manufacturer's instructions.

Anti-microtubule associated protein 2 (MAP2, Millipore, Billerica, MA; mouse monoclonal, SMI 52; #AB28032, dilution 1:1,000) is an IgG1 monoclonal antibody obtained from clone

SMI-52. SMI-52 specifically reacts with MAP2a and MAP2b protein isoforms, thus recognizes MAPs in neuronal cell bodies and dendrites. Immunoblot analysis recognizes a band at 280 kD, corresponding to MAP2a and b, and a doublet at 68 kDa, corresponding to MAP2c (technical information provided by Millipore).

The antibody against the homeobox transcription factor Phox2b was raised against the last 14 aa of the C-terminus of the Phox2b protein (Pattyn et al., 1997). The antibody specifically recognizes the Phox2b protein in mice and rats and does not crossreact with the homologous Phox2a protein; specificity was tested by lack of immunoreactivity in Phox2b null mice and identical expression pattern between immunohistochemistry and in situ hybridization data (Pattyn et al., 1997; Dauger et al., 2003; Stornetta et al., 2006; Kang et al., 2007).

The mouse monoclonal antiserum anti-parvalbumin (PV) (Sigma; #P3088; dilution 1:2,000), was prepared against a clone of the entire amino acid sequence of parvalbumin-19. This antibody specifically recognizes PV in human, bovine, goat, pig, dog, feline, rat, frog, and fish and does not react with other calcium-binding proteins such as calmodulin, intestinal calcium-binding protein, S100A2 (S100L), S100A6 (calcyclin), the α-chain of S-100 (i.e., in S-100a and S-100a_o), or the β-chain (i.e., in S-100a and S-100b), myosin light chain, and troponin (technical information provided by Sigma). In addition, the antibody does not crossreact with GABA, alanine, glycine, aspartate, taurine, carnosine, glutamine, glutamate, or calbindin. Celio and Heizmann (1981) demonstrated the specificity of the antibody by immunoprecipitating a single band (12 kDa) in total rat muscle extract and brain extract and immunostaining was abolished following preabsorption of the antiserum with the antigen. Our own data show a similar protein expression and localization in ventral respiratory column in adult rats, that is similar to what has been already published (Alheid et al., 2002).

Anti-EGFP was raised in chicken (Aves Labs, Tigard, OR; #GFP-1020, dilution 1:500) using purified recombinant EGFP emulsified in Freund's adjuvant as immunogen. The IgY fraction was purified from eggs. This anti-EGFP IgY specifically recognizes the viral-mediated EGFP-expressed neurons in adult rats (Tan et al., 2008). We observed lack of immunolabeling in tissue not infected with the virus.

The procedures for immunohistochemistry were described previously (Tan et al., 2008). Rats were anesthetized with Nembutal (100 mg kg^{-1}, i.p.) and perfused transcardially with 4% paraformaldehyde in PBS. The brainstem was removed and put in 4% paraformaldehyde/PBS for another 2 hours, followed by cryoprotection overnight in 30% sucrose in PBS. Forty-μm thick transverse sections were cut using a freezing microtome and incubated in primary antibodies described above, with 10% normal donkey serum for 24 or 48 hours at 4°C. Sst expression decreases with age (Hayashi et al., 1997; Lu et al., 2004). We found significantly more Sst-immunoreactive (-ir) neurons in preBötC in young compared to old rats. To facilitate detection of Sst-ir neurons in older rats (>300 g) we used a slightly different protocol. The rats (n = 4) were treated with 200 μg colchicine in 50 μL given into the cisterna magna for 24 hours before perfusion. The colchicine-treated animals were used for detection of colocalization of Sst and EGFP only. The animals without colchicine treatment were used to investigate colocalizations of EGFP and other molecular markers in brainstem. The brainstems were fixed in 4% paraformaldehyde/ PBS at 4°C overnight after transcardial perfusion, followed by cryoprotection overnight in 30% sucrose in PBS. Rabbit anti-Sst-14 (1:5,000) was incubated for 24 hours at 4°C and detected using the TSA/Tetramethyl-rhodamine system (Perkin Elmer, Waltham, MA). Other primary antibodies were detected by using the specific secondary antibodies (dilution 1:250): rhodamine-conjugated donkey antirabbit; rhodamine-conjugated donkey antimouse; and Cy5-conjugated donkey antirabbit secondary antibody were purchased from Jackson

ImmunoResearch Laboratories (West Grove, PA). Alexa 488-conjugated donkey anti-chicken was purchased from Invitrogen. Sections were then washed, mounted, and coverslipped.

Brainstem sections were grouped as one-in-six of sequential series of 40-μm transverse sections; thus, six groups of brainstem sections were collected from each rat and immunohistochemistry was performed using the following five groups of primary antibodies: Sst/EGFP, EGFP/MAP2, EGFP/NK1R, EGFP/PV, and EGFP/Phox2b. Images were acquired by confocal laser scanning microscopy (LSM510 META, Carl Zeiss, Heidenheim, Germany). For Alexa 488 and EGFP fluorescence, excitation (HeNe, 1 mV) was set to 488 nm, and emissions were gathered with a 500 –530 nm bandpass filter. For rhodamine fluorescence, excitation (HeNe, 1 mV) was set to 543 nm, and emissions were gathered with a 560-nm longpass filter. Z-stack images were acquired at 20X, 40X, or 63X magnification and images were exported to Adobe Illustrator (San Jose, CA) for figure composition. The images were cropped into suitable sizes without any other type of modification, such as contrast or brightness, etc.

RESULTS

Targeting preBötC neurons with an AAV2 virus

We used an AAV2 containing the Sst promoter driving EGFP expression to target a subpopulation of preBötC neurons (Tan et al., 2008). Three weeks after microinjection of the virus into the preBötC, EGFP expression was detectable and EGFP-expressing somas were limited in preBötC (Tan et al., 2008). The location of the preBötC was identified based on the distance from bregma, calamus scriptorius, and facial nucleus (Gray et al., 1999, 2001; Wang et al., 2001; Guyenet et al., 2002; Monnier et al., 2003). In all, 71% ± 6% of preBötC Sst neurons expressed EGFP and 67% ± 9% of the EGFP-expressing neurons were Sst neurons (n = 4; Fig. 1). Some EGFP-expressing processes from preBötC neurons on the injection side following unilateral injection were colocalized with MAP2, a major component of cross-bridges between microtubules in dendrites, indicating these processes were dendrites (Fig. 2). We found EGFP-expressing dendrites only on the injected side, covering the areas of preBötC, caudal BötC and rostral VRG (the region of the ventral respiratory group just caudal to the preBötC). We did not find EGFP-expressing cell bodies beyond these regions (Tan et al., 2008).

Projections to contralateral preBötC

In unilaterally injected rats, EGFP-expressing fibers crossed the midline at the level of preBötC and slightly rostral (Fig. 3A); some of these fibers could be followed to the contralateral preBötC. These fibers were not MAP2-ir, indicating that they were axons (Fig. 3). EGFP-expressing fibers project to contralateral preBötC (Fig. 4). These terminals were MAP2-ir-negative (data not shown). Some EGFP-expressing terminals were in juxtaposition to NK1R-ir neurons in the contralateral preBötC (Fig. 4).

Projections to BötC

A dense tract of EGFP-expressing axons projected to the ipsilateral (Fig. 5), and fewer to the contralateral, BötC. A few EGFP-expressing processes in the ipsilateral BötC were MAP2-ir (mainly in the most caudal portion; yellow arrow, Fig. 5 A–D), but the majority were MAP2-ir negative (white arrow, Fig. 5 A–D), suggesting that axons of preBötC Sst neurons projected bilaterally to or pass through the BötC, with only a few dendrites that extended rostrally into the ipsilateral caudal BötC. PV immunoreactivity identifies presumptive inhibitory bulbospinal neurons rostral (BötC) and caudal to the pre-BötC (Alheid et al., 2002). We could observe several EGFP terminals adjacent to PV-ir neurons and processes,

suggesting the occurrence of direct contacts of preBötC neurons on to PV BötC neurons (Fig. 5E–G).

Projections to VRC

The VRC caudal to the preBötC and extending until the spinal medullary junction contains bulbospinal premotor neurons that project mono- or oligo-synaptically to phrenic, intercostal, and abdominal motoneurons (Alheid et al., 2002). A massive tract of EGFP-expressing axons (MAP2-ir-negative), but no cell bodies, was found in the VRC in bilaterally injected rats (Fig. 6A, bottom box, 6C), suggesting the presence of axonal projections caudal to the preBötC.

Projections to parahypoglossal / NTS

A massive bundle of EGFP-expressing axons innervated the dorsal medulla in the region lateral to hypoglossal and ventral to NTS (Fig. 6A, top box, 6B), here referred to parahypoglossal/NTS. This region is involved in respiratory control: the parahypoglossal region contains premotor neurons that project to adjacent hypoglossal motoneurons (Dobbins and Feldman, 1995; Chamberlin et al., 2007), whereas the middle and caudal subnuclei of the NTS are a relay station for pulmonary vagal afferents (Kubin et al., 2006). From the injection site, EGFP-expressing axons ran caudally in the rVRG and cVRG (Fig. 6A, bottom box) and then routed dorsally toward the parahypoglossal/NTS region (Fig. 6A, top box). In unilaterally injected rats the majority of EGFP-expressing axons to the parahypoglossal/NTS were ipsilateral (data not shown).

Projections to retrotrapezoid nucleus/parafacial respiratory group (RTN/pFRG)

In unilaterally injected rats, EGFP-expressing axons projected bilaterally to the RTN/pFRG (Fig. 7). Phox2b is a transcription factor with nuclear localization and Phox2b-ir neurons are used to identify the pFRG/RTN (Stornetta et al., 2006; Lazarenko et al., 2009). Some EGFP-expressing terminals were close to Phox2b-ir neurons surrounding the facial nucleus on the ventral surface and medial to the facial nucleus, in the region that corresponds to the RTN/pFRG (Fig. 7). These results suggest synaptic contact between some EGFP-expressing terminals and Phox2b-ir neurons. On the ipsilateral side, more EGFP-expressing axons were found in the ventrolateral portion than in the ventromedial portion of this region, whereas on the contralateral side more EGFP-expressing axons were in the ventromedial portion than the ventrolateral portion, these terminals are MAP2-ir-negative (data not shown).

Projections to PB/KF

EGFP-expressing axons from the preBötC to the pons initially went rostrolaterally, and then moved dorsally toward the PB/KF (Fig. 8). In transverse section, these axons projected along the medial trigeminal tract in the lateral medulla (data not shown). Terminal fields were present on both sides of the PB/KF but were denser on the ipsilateral side.

Projections to PAG, raphé, cerebellum, and spinal cord

We observed some EGFP-expressing terminals in the lateral and ventrolateral PAG and raphé nucleus (data not shown). There were sparse EGFP-expressing terminals in the cerebellum and spinal cord at the cervical level (data not shown), suggesting projections. However, those EGFP-expressing terminals were too sparse to draw a reliable conclusion.

DISCUSSION

In adult rats we used AAV2 with the Sst promoter to express EGFP in a subpopulation of preBötC neurons (Tan et al., 2008) in order to map their brainstem projections. These

neurons, which when silenced in awake adult rats produces a profound long-lasting apnea, had extensive bilateral projections to multiple brainstem regions involved in the control of breathing including the VRG caudal to preBötC, pFRG/RTN, BötC, parahypoglossal/NTS, PB/KF, contralateral preBötC, and PAG (Fig. 9). We did not observe major projections to the cerebellum or spinal cord. We did not examine any other brain regions.

Technical considerations

Viruses used for tracing studies include different classes of adenovirus (Hermens et al., 1997) and herpes simplex virus (Breakefield and DeLuca, 1991); in our laboratory, using pseudorabies virus (PRV), we identified several premotoneuronal pools that innervate phrenic motoneurons (Dobbins and Feldman, 1994) or retractor or protruder hypoglossal motoneurons (Dobbins and Feldman, 1995).

AAVs can be used to identify specific phenotypes of neurons and their projections, with the significant advantage that they usually are not retrogradely transported (Klein et al., 1998; Chamberlin et al., 1998; Davidson et al., 2000), although some exceptions have been reported in the literature (Kaspar et al., 2002). Here, EGFP-expressing cell bodies were observed exclusively in the preBötC, confirming the absence of retrograde transport of the AAV2 virus from the injection site, and excluding the possibility that neurons outside of preBötC incorporated the virus due to the viral solution spreading.

Compared to chemical anterograde tracers, virally induced expression of EGFP as an anterograde tracer has several advantages:

1. Chemical tracers give a “smudgy” appearance at the injection site (Feil and Herbert, 1995), and nonneuronal cells, such as microglia, or axons of passage (Earle and Mitrofanis, 1997), can also take up, and in the case of axons, transport these tracers. Thus, it is very difficult to identify labeled neurons within the injection site that are filled with the tracers. In contrast, EGFP expressed in neurons infected with AAV2 is readily transported from the cell body to all dendrites and axons, illuminating their complete morphology and projections. In addition, EGFP is not released into the extracellular space, allowing for a fine analysis of the neurons infected by the virus at the injection site (Tan et al., 2008) as well as in terminal fields.
2. Long-term expression of EGFP in infected neurons of living animals allows one to track long axonal projections. In contrast, chemical anterograde tracers usually degrade and vanish from injection sites and labeled axons (Kobbert et al., 2000). Here, unilaterally and bilaterally injected rats did not show any respiratory disturbance or any other health problem for as long as 5 months postinjection (Tan et al., 2008), yet the intraneuronal labeling remained robust.
3. Chemical tracers do not select for different neuronal phenotypes; thus, a heterogeneous population is typically labeled. Using viruses that drive the expression of EGFP with proper promoters specific for a certain neuronal phenotype can restrict labeling to a spatially restricted phenotype of neurons and their projections.

True identity of neurons labeled with AAV2-SST-EGFP

One potential shortcoming of viral tracing is the leakage of cellular-specific promoter activity used in the viral vector, which may result in expression of EGFP in other phenotypic cells. Here the labeled neurons and their projections essentially overlap the population of neurons that when silenced produce profound apnea in awake adult rats (Pagliardini et al., 2003; Stornetta et al., 2003; Tan et al., 2008). In this study, most EGFP preBötC neurons

were Sst-ir-positive, while a small fraction were Sst-ir-negative. Determination of the degree to which the virally labeled neurons represent most, if not all, of preBötC neurons expressing Sst is beyond the scope of the present investigation. Thus, the projections presented here may not be solely from Sst preBötC neurons but also include projections from other preBötC neurons that do not express Sst. For the purposes of discussion, as in our previous article (Tan et al., 2008), we will assume that the data here are fully representative of projections from preBötC neurons expressing Sst.

Functional significance of projection network from preBötC Sst neurons

Sst is a tetradecapeptide first identified as an inhibitory regulator in the hypothalamus (Brazeau et al., 1973). As a powerful modulator of respiratory pattern (Kalia et al., 1984; Yamamoto et al., 1988), Sst is expressed in a subset of preBötC neurons (≈1,000) that partially overlap with NK1R neurons (Pagliardini et al., 2003; Stornetta et al., 2003; Tan et al., 2008). In infants who die of sudden infant death syndrome (SIDS) or sudden infant unexplained death (SIUD), there is a marked deficiency of preBötC neurons, including Sst neurons (Lavezzi and Matturri, 2008).

Acute silencing of preBötC Sst neurons produces a persistent apnea in awake adult rats (Tan et al., 2008). An essential element for understanding the role of these neurons in breathing is identifying their projections. Here we show that preBötC Sst neurons send projections to multiple respiratory-related nuclei throughout the brainstem. These projections suggest that the preBötC is able to modulate the activity of neurons in those nuclei, and these effects must be sufficiently vital that their suppression produces persistent apnea.

Contralateral preBötC—EGFP-expressing axons from each preBötC cross the midline at the preBötC and caudal BötC levels with some portion terminating in the contralateral preBötC, which is consistent with other studies (Koshiya and Smith, 1999; Stornetta et al., 2003). We cannot exclude the possibility that other preBötC neurons also project to contralateral preBötC. In rabbits and cats, respiratory rhythm continues after midline transection of the medulla but synchrony of left and right phrenic nerve activity is abolished, accompanied by a reduction in inspiratory motor output (Janczewski and Karczewski, 1984; Janczewski and Karczewski, 1990). This decussation of preBötC Sst axons may therefore play some roles in the bilateral symmetry of respiratory movements.

pFRG/RTN—The RTN is likely a key structure for central chemosensitivity (Smith et al., 1989; Connelly et al., 1990; Li and Nattie, 2002; Mulkey et al., 2004; Nattie and Li, 2008; Onimaru et al., 2008; Takakura et al., 2008; Lazarenko et al., 2009), providing an important drive to breathe, presumably by projections that include the one directed to the preBötC in rat (Ellenberger and Feldman, 1990) and cat (Smith et al., 1989). The pFRG lies in the same (general) region as the RTN (Janczewski et al., 2002), and they may overlap or be identical (Feldman et al., 2003; Stornetta et al., 2006; Onimaru et al., 2008; Guyenet et al., 2009). The pFRG/RTN has been postulated to contain neurons that are essential for active expiratory motor activity (Janczewski and Feldman, 2006; Abdala et al., 2009). Some RTN neurons in anesthetized restrained rats receive a respiratory-modulated inhibitory projection (Guyenet et al., 2005). Whether the projections found in this study are excitatory or inhibitory needs further investigation. Nevertheless, preBötC Sst neurons strongly project to the pFRG/RTN, providing an anatomical substrate for interactions with its chemosensory and rhythmogenic elements that could contribute to the coordination of inspiratory and expiratory activity.

BötC—The BötC contains mainly glycinergic neurons, some of which modulate activity of phrenic premotor neurons in the VRG (Dobbins and Feldman, 1994; Ezure et al., 2003). BötC expiratory neurons have a role in synchronizing respiratory timing by suppressing

inspiratory neurons (Fedorko and Merrill, 1984) and preventing improper activation of inspiratory muscles during expiration (Feldman, 1986). BötC expiratory inhibitory neurons project either to the caudal VRG or directly to the phrenic nucleus. We found a few EGFP-expressing fibers in BötC bilaterally, suggesting the existence of projections from preBötC Sst neurons to BötC.

VRG caudal to preBötC—Caudal to the preBötC are premotor neurons grouped in two major subdivisions: the rostral VRG, which contains inspiratory bulbospinal neurons that project to the phrenic and intercostal nuclei (Feldman, 1986; Ellenberger and Feldman, 1990; Dobbins and Feldman, 1994), and the caudal VRG, which contains mainly expiratory premotor neurons projecting to internal intercostal and abdominal motoneurons (Ellenberger et al., 1990). Massive projections from the preBötC bilaterally to the rVRG and cVRG suggest that the premotor neurons in these regions receive strong inspiratory drive from preBötC Sst neurons that they in turn transmit to spinal cord inspiratory and expiratory motoneurons.

Parahypoglossal/NTS—The NTS is an important relay station for visceral sensory information. The caudomedial NTS receives lung stretch receptor afferents (Kubin et al., 2006). In cat, the ventrolateral NTS projects to the phrenic nucleus (Fedorko et al., 1983; Feldman, 1986; Ezure, 1990), but this projection, if it exists, is much weaker in rat (Onai et al., 1987; Yamada et al., 1988; Ezure et al., 1988; Hilaire et al., 1990). In our study we identify projections from the preBötC Sst neurons directed mainly to the ventrolateral and the medial subnuclei of the caudal NTS where inspiratory neurons are found in rats (Saether et al., 1987; Bonham and McCrimmon, 1990). This suggests that the preBötC can affect integration of inspiratory drive with sensory input within the NTS.

When PRV is injected into protruder and retractor muscles of the tongue in rats, premotor neurons are bilaterally labeled ventral to NTS and lateral to dorsal hypoglossal nucleus, as well as the ventral, interstitial, and medial NTS (Dobbins and Feldman, 1995). preBötC Sst neurons project to these regions. Collectively, our study and previous reports (Dobbins and Feldman, 1995; Chamberlin et al., 2007) suggest that the parahypoglossal/NTS contains premotor neurons for hypoglossal motor neurons, and they receive direct input from preBötC neurons.

PB/KF—The PB/KF is involved in respiratory control and modulation (Cohen and Wang, 1959; Feldman, 1986). These structures contain three major respiratory-related neuronal populations: 1) inspiratory neurons with an augmenting discharge pattern; 2) postinspiratory neurons; and 3) inspiratory-expiratory phase-spanning neurons (Cohen and Wang, 1959; Feldman and Gautier, 1976; Feldman, 1986; Ezure, 2004). Stimulation of PB/KF may facilitate or inhibit respiration, depending on which subpopulations are stimulated (Cohen, 1971; Chamberlin and Saper, 1994). The PB/KF plays a role in termination of the inspiratory phase and control of expiratory duration (von Euler et al., 1976; Feldman et al., 1992; Oku and Dick, 1992). The PB/KF receives projections from and projects to medullary respiratory-related nuclei, including the NTS, VRG, and hypoglossal nucleus (Smith et al., 1989; Herbert et al., 1990; Ellenberger and Feldman, 1990; Gang et al., 1998; Ezure and Tanaka, 2006). Here we show that preBötC Sst neurons project to the PB/KF, potentially a source of their respiratory-modulated activity.

PAG—The PAG is involved in vocalization and respiration (Bandler et al., 1991; Davis et al., 1996). Stimulation of the PAG can modulate breathing (Kabat, 1936; Subramanian et al., 2008). Furthermore, activation of caudal dorsal PAG reveals greater respiratory responses than rostral dorsal PAG stimulation (Zhang et al., 2007). The PAG projects to pontine

respiratory group, ventrolateral medulla, and NTS (Cameron et al., 1995). We found that preBötC neurons have direct projections to the lateral and ventrolateral PAG. Stimulations in these areas induce tachypnea and apneusis in cats (Subramanian et al., 2008). These results suggest reciprocal connections between these regions. The phenotypes of PAG neurons that receive the projections need further determination. These projections suggest the preBötC may be involved in modulating the function of the PAG.

Sst modulation of breathing

Sst is a powerful neuropeptide modulator of breathing (Kalia et al., 1984; Yamamoto et al., 1988; Chen et al., 1990). Sst had no effect on respiration when administered into the lateral ventricle (ICV) (Niewoehner et al., 1983); however, *icc* administration of Sst can induce irreversible apnea in anesthetized rats (Kalia et al., 1984). The molecular pathways, the pharmacology, and anatomical targets of Sst action on the respiratory network are still unknown. Here we show that preBötC Sst neurons send projections to multiple respiratory-related structures located in the VRG and in the dorsal brainstem, including regions containing premotor neurons of the XII, the NTS, and the PB/KF.

Sst also affects chemosensory drive. For instance, the latency of Sst-induced apnea is shortened by hypoxia or hypercapnia in vivo (Harfstrand et al., 1984). Acidification potentiates the Sst-induced suppression of inspiration in the medullary-spinal cord preparation in vitro (Llona et al., 2004). As Sst was administrated into whole medulla in these studies, how Sst regulates the chemosensory drive could not be determined. Our results raise the possibility that Sst may act on RTN neurons directly affecting chemosensory drive.

Functional impairment of Sst neurons in respiratory-related diseases

Disruption of Sst neurons may underlie respiratory disturbances in several perinatal and neurodegenerative diseases. In infants who die of SIDS or SIUD, there is a marked deficiency of preBötC neurons, including Sst neurons (Lavezzi and Matturri, 2008); preBötC Sst neurons degeneration has also been reported in multiple systemic atrophy patients (Schwarzacher, 2007); in addition, Sst neuron loss is present at the early stages and possibly a critical event in the process of Alzheimer's disease (AD) (Davies et al., 1980; Roberts et al., 1985) since Sst may modulate the accumulation of amyloid β peptide (Aβ) through upregulation of neprilysin-mediated proteolytic degradation (Saito et al., 2005). AD patients commonly suffer poor sleep with a high reported incidence of sleep-disordered breathing (SDB). Mild to moderate AD patients with SDB spend less of the night in REM sleep than those without SDB (Cooke et al., 2006). These data are consistent with our previous report that progressive ablation of preBötC in rats causes sustained and repeated apneas that first appear during REM sleep and then progressively in NREM and awake states (McKay et al., 2005). Impairment of preBötC function in AD, caused by changes of excitability and/or loss of Sst and/or NK1R neurons, could result in central sleep apnea (McKay et al., 2005), or even respiratory failure in the late stages of the diseases. During slow neurodegeneration in preBötC, compensatory mechanisms might resolve apnea in wakefulness (McKay et al., 2005). However, the compensatory pathway is very fragile when the depression of preBötC Sst neurons is sudden, which may provide insight into mechanisms of sudden respiratory failure in some cases of SIDS and SUID and of central sleep apnea.

Our results here show that preBötC Sst neurons send their projections to most of respiratory-related nuclei in the brainstem, implying that loss of these neurons could contribute to, and even be the principal cause of, the disruption of normal breathing in these pathologies.

Supplementary Material

Refer to Web version on PubMed Central for supplementary material.

Acknowledgments

We thank Grace Li and Peter Liu for histological assistance.

Grant sponsor: National Institutes of Health; Grant numbers: HL70029 and HL94811; Grant sponsor: Alberta Heritage Foundation for Medical Research (post-doctoral fellowship to S.P.); Grant sponsor: Canadian Institute of Health Research (grant to S.P.).

LITERATURE CITED

Abdala AP, Rybak IA, Smith JC, Paton JF. Abdominal expiratory activity in the rat brainstem-spinal cord in situ: patterns, origins and implications for respiratory rhythm generation. J Physiol. 2009; 587(Pt 14):3539–3559. [PubMed: 19491247]

Alheid GF, Gray PA, Jiang MC, Feldman JL, McCrimmon DR. Parvalbumin in respiratory neurons of the ventrolateral medulla of the adult rat. J Neurocytol. 2002; 31:693–717. [PubMed: 14501208]

Bandler R, Carrive P, Zhang SP. Integration of somatic and autonomic reactions within the midbrain periaqueductal grey: viscerotopic, somatotopic and functional organization. Prog Brain Res. 1991; 87:269–305. [PubMed: 1678189]

Bonham AC, McCrimmon DR. Neurones in a discrete region of the nucleus tractus solitarius are required for the Breuer-Hering reflex in rat. J Physiol. 1990; 427:261–280. [PubMed: 2213599]

Brazeau P, Vale W, Burgus R, Ling N, Butcher M, Rivier J, Guillemin R. Hypothalamic polypeptide that inhibits the secretion of immunoreactive pituitary growth hormone. Science. 1973; 179:77–79. [PubMed: 4682131]

Breakefield XO, DeLuca NA. Herpes simplex virus for gene delivery to neurons. New Biologist. 1991; 3:203–218. [PubMed: 1652278]

Cameron AA, Khan IA, Westlund KN, Willis WD. The efferent projections of the periaqueductal gray in the rat: a Phaseolus vulgaris-leucoagglutinin study. II. Descending projections. J Comp Neurol. 1995; 351:585–601. [PubMed: 7721985]

Celio MR, Heizmann CW. Calcium-binding protein parvalbumin as a neuronal marker. Nature. 1981; 293:300–302. [PubMed: 7278987]

Chamberlin NL, Saper CB. Topographic organization of respiratory responses to glutamate microstimulation of the parabrachial nucleus in the rat. J Neurosci. 1994; 14(11 Pt 1):6500–6510. [PubMed: 7965054]

Chamberlin NL, Du B, de Lacalle S, Saper CB. Recombinant adeno-associated virus vector: use for transgene expression and anterograde tract tracing in the CNS. Brain Res. 1998; 793:169–175. [PubMed: 9630611]

Chamberlin NL, Eikermann M, Fassbender P, White DP, Malhotra A. Genioglossus premotoneurons and the negative pressure reflex in rats. J Physiol. 2007; 579(Pt 2):515–526. [PubMed: 17185342]

Chen ZB, Hedner T, Hedner J. Local application of somatostatin in the rat ventrolateral brain medulla induces apnea. J Appl Physiol. 1990; 69:2233–2238. [PubMed: 1981770]

Cohen MI. Switching of the respiratory phases and evoked phrenic responses produced by rostral pontine electrical stimulation. J Physiol. 1971; 217:133–158. [PubMed: 5571915]

Cohen MI, Wang SC. Respiratory neuronal activity in pons of cat. J Neurophysiol. 1959; 22:33–50. [PubMed: 13621254]

Connelly CA, Ellenberger HH, Feldman JL. Respiratory activity in retrotrapezoid nucleus in cat. Am J Physiol. 1990; 258(2 Pt 1):L33–44. [PubMed: 2305898]

Cooke JR, Liu L, Natarajan L, He F, Marler M, Loredo JS, Corey-Bloom J, Palmer BW, Greenfield D, Ancoli-Israel S. The effect of sleep-disordered breathing on stages of sleep in patients with Alzheimer's disease. Behav Sleep Med. 2006; 4:219–227. [PubMed: 17083302]

Dauger S, Pattyn A, Lofaso F, Gaultier C, Goridis C, Gallego J, Brunet JF. Phox2b controls the development of peripheral chemoreceptors and afferent visceral pathways. Development. 2003; 130:6635–6642. [PubMed: 14627719]

Davidson BL, Stein CS, Heth JA, Martins I, Kotin RM, Derksen TA, Zabner J, Ghodsi A, Chiorini JA. Recombinant adeno-associated virus type 2, 4, and 5 vectors: transduction of variant cell types and regions in the mammalian central nervous system. Proc Natl Acad Sci U S A. 2000; 97:3428–3432. [PubMed: 10688913]

Davies P, Katzman R, Terry RD. Reduced somatostatin-like immunoreactivity in cerebral cortex from cases of Alzheimer disease and Alzheimer senile dementia. Nature. 1980; 288:279–280. [PubMed: 6107862]

Davis PJ, Zhang SP, Winkworth A, Bandler R. Neural control of vocalization: respiratory and emotional influences. J Voice. 1996; 10:23–38. [PubMed: 8653176]

Dobbins EG, Feldman JL. Brainstem network controlling descending drive to phrenic motoneurons in rat. J Comp Neurol. 1994; 347:64–86. [PubMed: 7798382]

Dobbins EG, Feldman JL. Differential innervation of protruder and retractor muscles of the tongue in rat. J Comp Neurol. 1995; 357:376–394. [PubMed: 7673474]

Earle KL, Mitrofanis J. Identification of transient microglial cell colonies in the forebrain white matter of developing rats. J Comp Neurol. 1997; 387:371–384. [PubMed: 9335421]

Ellenberger HH, Feldman JL. Brainstem connections of the rostral ventral respiratory group of the rat. Brain Res. 1990; 513:35–42. [PubMed: 2350683]

Ellenberger HH, Feldman JL, Zhan WZ. Subnuclear organization of the lateral tegmental field of the rat. II: Catecholamine neurons and ventral respiratory group. J Comp Neurol. 1990; 294:212–222. [PubMed: 2332529]

Ezure K. Synaptic connections between medullary respiratory neurons and considerations on the genesis of respiratory rhythm. Prog Neurobiol. 1990; 35:429–450. [PubMed: 2175923]

Ezure K. Respiration-related afferents to parabrachial pontine regions. Respir Physiol Neurobiol. 2004; 143:167–175. [PubMed: 15519553]

Ezure K, Tanaka I. Distribution and medullary projection of respiratory neurons in the dorsolateral pons of the rat. Neuroscience. 2006; 141:1011–1023. [PubMed: 16725272]

Ezure K, Manabe M, Yamada H. Distribution of medullary respiratory neurons in the rat. Brain Res. 1988; 455:262–270. [PubMed: 3401782]

Ezure K, Tanaka I, Kondo M. Glycine is used as a transmitter by decrementing expiratory neurons of the ventrolateral medulla in the rat. J Neurosci. 2003; 23:8941–8948. [PubMed: 14523096]

Fedorko L, Merrill EG. Axonal projections from the rostral expiratory neurones of the Botzinger complex to medulla and spinal cord in the cat. J Physiol. 1984; 350:487–496. [PubMed: 6747857]

Fedorko L, Merrill EG, Lipski J. Two descending medullary inspiratory pathways to phrenic motoneurones. Neurosci Lett. 1983; 43:285–291. [PubMed: 6672694]

Feil K, Herbert H. Topographic organization of spinal and trigeminal somatosensory pathways to the rat parabrachial and Kolliker-Fuse nuclei. J Comp Neurol. 1995; 353:506–528. [PubMed: 7759613]

Feldman, JL. Handbook of physiology, Section 1. The nervous system. In: Bloom, FE., editor. Neurophysiology of breathing in mammals. Bethesda, MD: American Physiology Society; 1986. p. 463-524.

Feldman JL, Del Negro CA. Looking for inspiration: new perspectives on respiratory rhythm. Nat Rev Neurosci. 2006; 7:232–242. [PubMed: 16495944]

Feldman JL, Gautier H. Interaction of pulmonary afferents and pneumotaxic center in control of respiratory pattern in cats. J Neurophysiol. 1976; 39:31–44. [PubMed: 1249602]

Feldman JL, Windhorst U, Anders K, Richter DW. Synaptic interaction between medullary respiratory neurones during apneusis induced by NMDA-receptor blockade in cat. J Physiol. 1992; 450:303–323. [PubMed: 1432710]

Feldman JL, Mitchell GS, Nattie EE. Breathing: rhythmicity, plasticity, chemosensitivity. Annu Rev Neurosci. 2003; 26:239–266. [PubMed: 12598679]

Gang S, Watanabe A, Aoki M. Axonal projections from the pontine parabrachial-Kolliker-Fuse nuclei to the Botzinger complex as revealed by antidromic stimulation in cats. Adv Exp Med Biol. 1998; 450:67–72. [PubMed: 10026965]

Gray PA, Rekling JC, Bocchiaro CM, Feldman JL. Modulation of respiratory frequency by peptidergic input to rhythmogenic neurons in the preBotzinger complex. Science. 1999; 286:1566–1568. [PubMed: 10567264]

Gray PA, Janczewski WA, Mellen N, McCrimmon DR, Feldman JL. Normal breathing requires preBotzinger complex neurokinin-1 receptor-expressing neurons. Nat Neurosci. 2001; 4:927–930. [PubMed: 11528424]

Guyenet PG, Sevigny CP, Weston MC, Stornetta RL. Neurokinin-1 receptor-expressing cells of the ventral respiratory group are functionally heterogeneous and predominantly glutamatergic. J Neurosci. 2002; 22:3806–3816. [PubMed: 11978856]

Guyenet PG, Mulkey DK, Stornetta RL, Bayliss DA. Regulation of ventral surface chemoreceptors by the central respiratory pattern generator. J Neurosci. 2005; 25:8938–8947. [PubMed: 16192384]

Guyenet PG, Bayliss DA, Stornetta RL, Fortuna MG, Abbott SB, DePuy SD. Retrotrapezoid nucleus, respiratory chemosensitivity and breathing automaticity. Respir Physiol Neurobiol. 2009; 168:59–68. [PubMed: 19712903]

Harfstrand A, Kalia M, Fuxe K, Kaijser L, Agnati LF. Somatostatin-induced apnea: interaction with hypoxia and hypercapnea in the rat. Neurosci Lett. 1984; 50:37–42. [PubMed: 6149505]

Hayashi M, Yamashita A, Shimizu K. Somatostatin and brain-derived neurotrophic factor mRNA expression in the primate brain: decreased levels of mRNAs during aging. Brain Res. 1997; 749:283–289. [PubMed: 9138728]

Herbert H, Moga MM, Saper CB. Connections of the parabrachial nucleus with the nucleus of the solitary tract and the medullary reticular formation in the rat. J Comp Neurol. 1990; 293:540–580. [PubMed: 1691748]

Hermens WT, Giger RJ, Holtmaat AJ, Dijkhuizen PA, Houweling DA, Verhaagen J. Transient gene transfer to neurons and glia: analysis of adenoviral vector performance in the CNS and PNS. J Neurosci Methods. 1997; 71:85–98. [PubMed: 9125378]

Hilaire G, Monteau R, Gauthier P, Rega P, Morin D. Functional significance of the dorsal respiratory group in adult and newborn rats: in vivo and in vitro studies. Neurosci Lett. 1990; 111:133–138. [PubMed: 2336178]

Janczewski WA, Feldman JL. Distinct rhythm generators for inspiration and expiration in the juvenile rat. J Physiol. 2006; 570(Pt 2):407–420. [PubMed: 16293645]

Janczewski WA, Karczewski WA. Respiratory effects of pontine, medullary and spinal cord midline sections in the rabbit. Respir Physiol. 1984; 57:293–305. [PubMed: 6522867]

Janczewski WA, Karczewski WA. The role of neural connections crossed at the cervical level in determining rhythm and amplitude of respiration in cats and rabbits. Respir Physiol. 1990; 79:163–175. [PubMed: 2336493]

Janczewski WA, Onimaru H, Homma I, Feldman JL. Opioid-resistant respiratory pathway from the preinspiratory neurones to abdominal muscles: in vivo and in vitro study in the newborn rat. J Physiol. 2002; 545(Pt 3):1017–1026. [PubMed: 12482904]

Kabat H. Electrical stimulation of points in the forebrain and midbrain: the resultant alternations in respiration. J Comp Neurol. 1936; 64:187–208.

Kalia M, Fuxe K, Agnati LF, Hokfelt T, Harfstrand A. Somatostatin produces apnea and is localized in medullary respiratory nuclei: a possible role in apneic syndromes. Brain Res. 1984; 296:339–344. [PubMed: 6142757]

Kang BJ, Chang DA, Mackay DD, West GH, Moreira TS, Takakura AC, Gwilt JM, Guyenet PG, Stornetta RL. Central nervous system distribution of the transcription factor Phox2b in the adult rat. J Comp Neurol. 2007; 503:627–641. [PubMed: 17559094]

Kaspar BK, Erickson D, Schaffer D, Hinh L, Gage FH, Peterson DA. Targeted retrograde gene delivery for neuronal protection. Mol Ther. 2002; 5:50–56. [PubMed: 11786045]

Klein RL, Meyer EM, Peel AL, Zolotukhin S, Meyers C, Muzyczka N, King MA. Neuron-specific transduction in the rat septohippocampal or nigrostriatal pathway by recombinant adeno-associated virus vectors. Exp Neurol. 1998; 150:183–194. [PubMed: 9527887]

Kobbert C, Apps R, Bechmann I, Lanciego JL, Mey J, Thanos S. Current concepts in neuroanatomical tracing. Prog Neurobiol. 2000; 62:327–351. [PubMed: 10856608]

Koshiya N, Smith JC. Neuronal pacemaker for breathing visualized in vitro. Nature. 1999; 400:360–363. [PubMed: 10432113]

Kubin L, Alheid GF, Zuperku EJ, McCrimmon DR. Central pathways of pulmonary and lower airway vagal afferents. J Appl Physiol. 2006; 101:618–627. [PubMed: 16645192]

Lavezzi A, Matturri L. Functional neuroanatomy of the human pre-Botzinger complex with particular reference to sudden unexplained perinatal and infant death. Neuropathology. 2008; 28:10–16. [PubMed: 18031468]

Lazarenko RM, Milner TA, Depuy SD, Stornetta RL, West GH, Kievits JA, Bayliss DA, Guyenet PG. Acid sensitivity and ultrastructure of the retrotrapezoid nucleus in Phox2b-EGFP transgenic mice. J Comp Neurol. 2009; 517:69–86. [PubMed: 19711410]

Li A, Nattie E. CO2 dialysis in one chemoreceptor site, the RTN: stimulus intensity and sensitivity in the awake rat. Respir Physiol Neurobiol. 2002; 133:11–22. [PubMed: 12385727]

Llona I, Ampuero E, Eugenin JL. Somatostatin inhibition of fictive respiration is modulated by pH. Brain Res. 2004; 1026:136–142. [PubMed: 15476705]

Lu T, Pan Y, Kao SY, Li C, Kohane I, Chan J, Yankner BA. Gene regulation and DNA damage in the ageing human brain. Nature. 2004; 429:883–891. [PubMed: 15190254]

Mantyh PW, Rogers SD, Honore P, Allen BJ, Ghilardi JR, Li J, Daughters RS, Lappi DA, Wiley RG, Simone DA. Inhibition of hyperalgesia by ablation of lamina I spinal neurons expressing the substance P receptor. Science. 1997; 278:275–279. [PubMed: 9323204]

McKay LC, Janczewski WA, Feldman JL. Sleep-disordered breathing after targeted ablation of preBotzinger complex neurons. Nat Neurosci. 2005; 8:1142–1144. [PubMed: 16116455]

Monnier A, Alheid GF, McCrimmon DR. Defining ventral medullary respiratory compartments with a glutamate receptor agonist in the rat. J Physiol. 2003; 548(Pt 3):859–874. [PubMed: 12640009]

Mulkey DK, Stornetta RL, Weston MC, Simmons JR, Parker A, Bayliss DA, Guyenet PG. Respiratory control by ventral surface chemoreceptor neurons in rats. Nat Neurosci. 2004; 7:1360–1369. [PubMed: 15558061]

Nattie G, Li A. Multiple central chemoreceptor sites: cell types and function in vivo. Adv Exp Med Biol. 2008; 605:343–347. [PubMed: 18085297]

Niewoehner DE, Levine AS, Morley JE. Central effects of neuropeptides on ventilation in the rat. Peptides. 1983; 4:277–281. [PubMed: 6195647]

Oku Y, Dick TE. Phase resetting of the respiratory cycle before and after unilateral pontine lesion in cat. J Appl Physiol. 1992; 72:721–730. [PubMed: 1559953]

Onai T, Saji M, Miura M. Projections of supraspinal structures to the phrenic motor nucleus in rats studied by a horse-radish peroxidase microinjection method. J Auton Nerv Syst. 1987; 21:233–239. [PubMed: 2836492]

Onimaru H, Ikeda K, Kawakami K. CO2-sensitive preinspiratory neurons of the parafacial respiratory group express Phox2b in the neonatal rat. J Neurosci. 2008; 28:12845–12850. [PubMed: 19036978]

Pagliardini S, Ren J, Greer JJ. Ontogeny of the pre-Botzinger complex in perinatal rats. J Neurosci. 2003; 23:9575–9584. [PubMed: 14573537]

Pagliardini S, Adachi T, Ren J, Funk GD, Greer JJ. Fluorescent tagging of rhythmically active respiratory neurons within the pre-Botzinger complex of rat medullary slice preparations. J Neurosci. 2005; 25:2591–2596. [PubMed: 15758169]

Pattyn A, Morin X, Cremer H, Goridis C, Brunet JF. Expression and interactions of the two closely related homeobox genes Phox2a and Phox2b during neurogenesis. Development. 1997; 124:4065–4075. [PubMed: 9374403]

Roberts GW, Crow TJ, Polak JM. Location of neuronal tangles in somatostatin neurones in Alzheimer's disease. Nature. 1985; 314:92–94. [PubMed: 2858057]

Saether K, Hilaire G, Monteau R. Dorsal and ventral respiratory groups of neurons in the medulla of the rat. Brain Res. 1987; 419:87–96. [PubMed: 3676744]

Saito T, Iwata N, Tsubuki S, Takaki Y, Takano J, Huang SM, Suemoto T, Higuchi M, Saido TC. Somatostatin regulates brain amyloid beta peptide Abeta42 through modulation of proteolytic degradation. Nat Med. 2005; 11:434–439. [PubMed: 15778722]

Schwarzacher, SW.; Rub, U.; Bohl, J.; Brunt, ER.; Deller, T. The human pre-Boetzinger Complex. 37th Annual Meeting of the Society of Neuroscience; San Diego, CA. 2007.

Smith JC, Morrison DE, Ellenberger HH, Otto MR, Feldman JL. Brainstem projections to the major respiratory neuron populations in the medulla of the cat. J Comp Neurol. 1989; 281:69–96. [PubMed: 2466879]

Smith JC, Ellenberger HH, Ballanyi K, Richter DW, Feldman JL. Pre-Botzinger complex: a brainstem region that may generate respiratory rhythm in mammals. Science. 1991; 254:726–729. [PubMed: 1683005]

Stornetta RL, Rosin DL, Wang H, Sevigny CP, Weston MC, Guyenet PG. A group of glutamatergic interneurons expressing high levels of both neurokinin-1 receptors and somatostatin identifies the region of the pre-Botzinger complex. J Comp Neurol. 2003; 455:499–512. [PubMed: 12508323]

Stornetta RL, Moreira TS, Takakura AC, Kang BJ, Chang DA, West GH, Brunet JF, Mulkey DK, Bayliss DA, Guyenet PG. Expression of Phox2b by brainstem neurons involved in chemosensory integration in the adult rat. J Neurosci. 2006; 26:10305–10314. [PubMed: 17021186]

Subramanian HH, Balnave RJ, Holstege G. The midbrain periaqueductal gray control of respiration. J Neurosci. 2008; 28:12274–12283. [PubMed: 19020021]

Takakura AC, Moreira TS, Stornetta RL, West GH, Gwilt JM, Guyenet PG. Selective lesion of retrotrapezoid Phox2b-expressing neurons raises the apnoeic threshold in rats. J Physiol. 2008; 586(Pt 12):2975–2991. [PubMed: 18440993]

Tan EM, Yamaguchi Y, Horwitz GD, Gosgnach S, Lein ES, Goulding M, Albright TD, Callaway EM. Selective and quickly reversible inactivation of mammalian neurons in vivo using the Drosophila allatostatin receptor. Neuron. 2006; 51:157–170. [PubMed: 16846851]

Tan W, Janczewski WA, Yang P, Shao XM, Callaway EM, Feldman JL. Silencing preBotzinger complex somatostatin-expressing neurons induces persistent apnea in awake rat. Nat Neurosci. 2008; 11:538–540. [PubMed: 18391943]

Vigna SR, Bowden JJ, McDonald DM, Fisher J, Okamoto A, McVey DC, Payan DG, Bunnett NW. Characterization of antibodies to the rat substance P (NK-1) receptor and to a chimeric substance P receptor expressed in mammalian cells. J Neurosci. 1994; 14:834–845. [PubMed: 7507985]

von Euler C, Marttila I, Remmers JE, Trippenbach T. Effects of lesions in the parabrachial nucleus on the mechanisms for central and reflex termination of inspiration in the cat. Acta Physiol Scand. 1976; 96:324–337. [PubMed: 1274615]

Wang H, Stornetta RL, Rosin DL, Guyenet PG. Neurokinin-1 receptor-immunoreactive neurons of the ventral respiratory group in the rat. J Comp Neurol. 2001; 434:128–146. [PubMed: 11331521]

Yamada H, Ezure K, Manabe M. Efferent projections of inspiratory neurons of the ventral respiratory group. A dual labeling study in the rat. Brain Res. 1988; 455:283–294. [PubMed: 3401784]

Yamamoto Y, Runold M, Prabhakar N, Pantaleo T, Lagercrantz H. Somatostatin in the control of respiration. Acta Physiol Scand. 1988; 134:529–533. [PubMed: 2907961]

Zhang W, Hayward LF, Davenport PW. Respiratory responses elicited by rostral versus caudal dorsal periaqueductal gray stimulation in rats. Auton Neurosci. 2007; 134:45–54. [PubMed: 17363338]

Zolotukhin S, Byrne BJ, Mason E, Zolotukhin I, Potter M, Chesnut K, Summerford C, Samulski RJ, Muzyczka N. Recombinant adeno-associated virus purification using novel methods improves infectious titer and yield. Gene Ther. 1999; 6:973–985. [PubMed: 10455399]

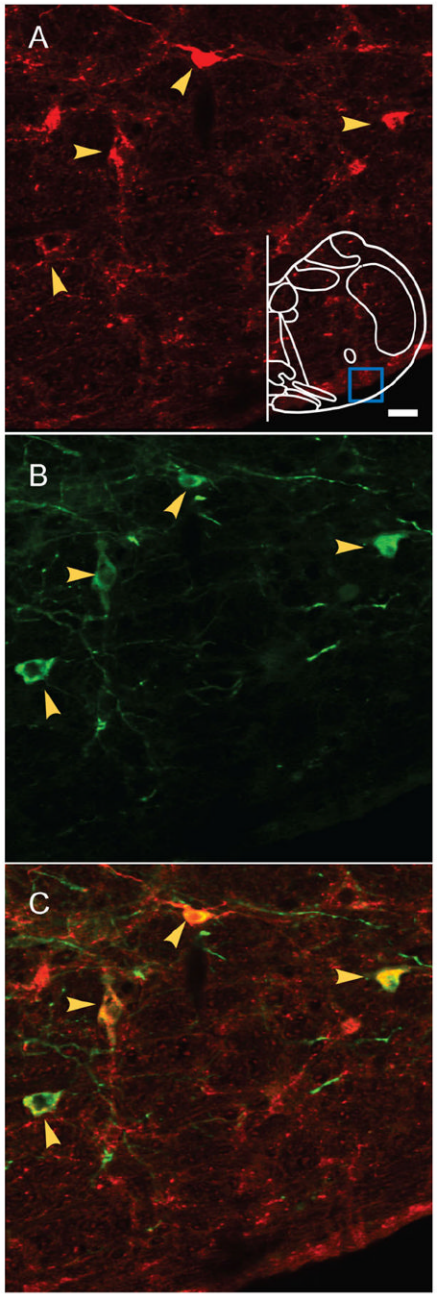

Figure 1. AAV2 viral targeting of preBötC Sst neurons

Double immunostaining of Sst and EGFP shows the colocalization of both markers in preBötC. **A:** Sst-ir neurons. Blue box in outline represents area where images were acquired. **B:** EGFP-ir neurons. **C:** Colocalization of both markers indicated by yellow arrows. Magenta-green copy of this figure is available as Supporting Figure 1. Scale bar = 20 μm. [Color figure can be viewed in the online issue, which is available at www.interscience.wiley.com.]

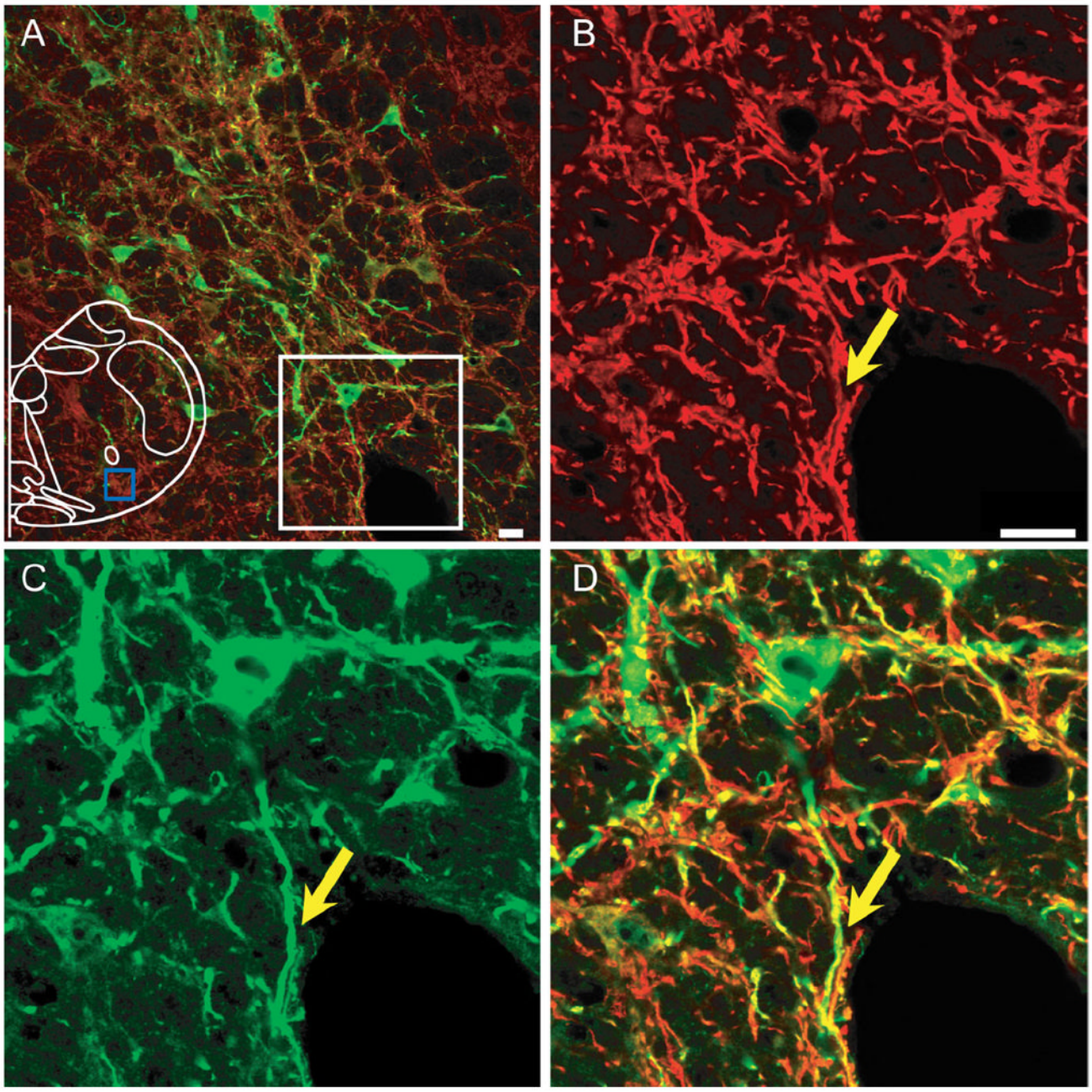

Figure 2. EGFP is expressed in dendrites of transfected preBötC neurons

A: EGFP expression in somas and processes in preBötC on injected side of unilaterally injected rats. Some EGFP-expressing fibers (green) colocalized with MAP2-ir processes (red). Blue box in outline represents area where images were acquired. **B–D:** Higher magnification of immunoreactivity for MAP2 (B), EGFP (C), and overlapping images (D) from the white box in (A). Yellow arrow indicates colocalization of EGFP and MAP2. Magenta-green copy of this figure is available as Supporting Figure 2. Scale bar = 20 μm. [Color figure can be viewed in the online issue, which is available at www.interscience.wiley.com.]

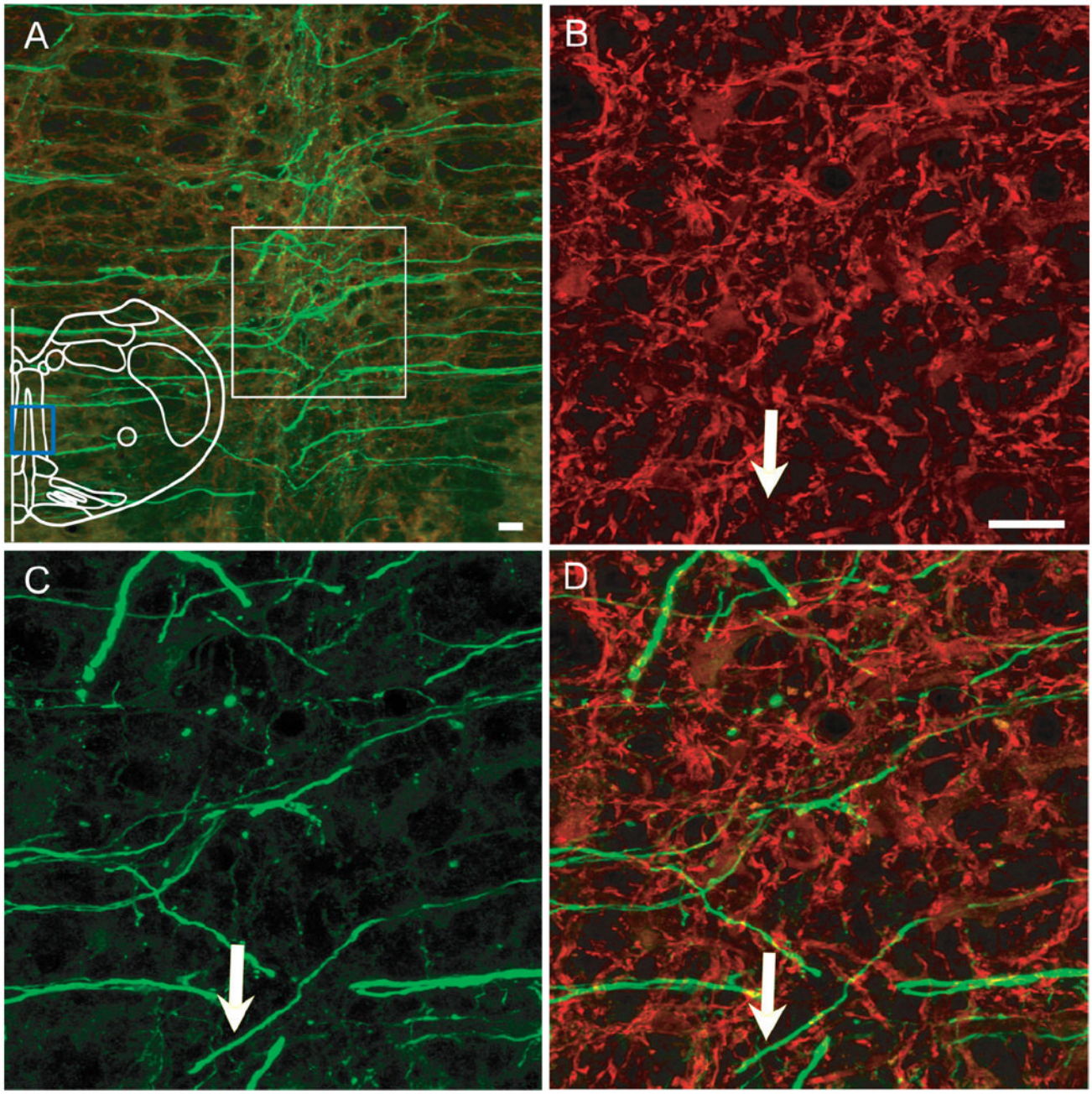

Figure 3. Axons from preBötC Sst neurons cross the midline

A: Axons cross the midline and project to contralateral side brainstem after unilateral injection. Blue box in outline represents area where images were acquired. **B–D:** Higher magnification of immunoreactivity for MAP2 (B), EGFP (C), and overlap (D) from white box in (A). EGFP and MAP2 were not colocalized, e.g., white arrow. Magenta-green copy of this figure is available as Supporting Figure 3. Scale bar = 20 μm. [Color figure can be viewed in the online issue, which is available at www.interscience. wiley.com.]

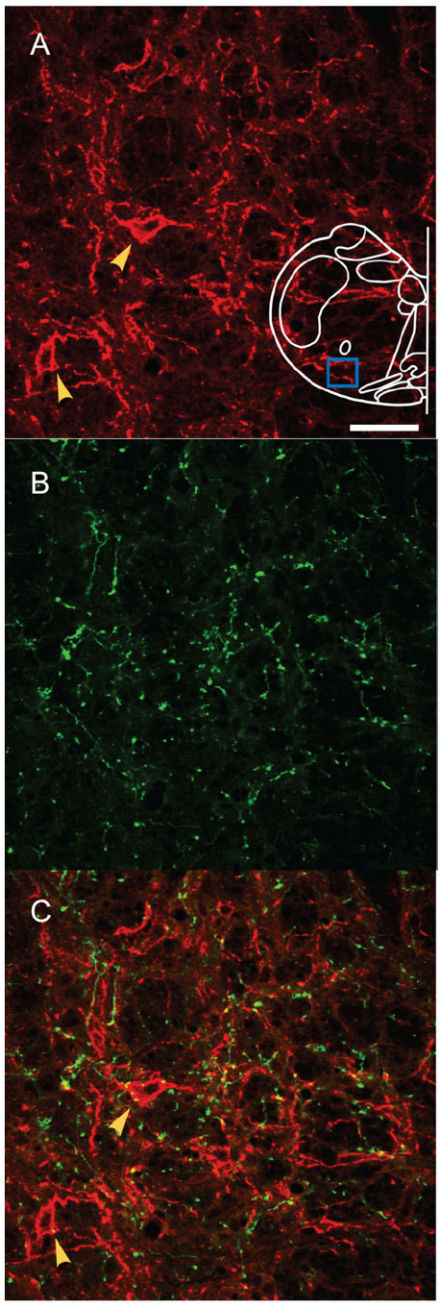

Figure 4. Projections to contralateral preBötC after unilateral injection

A: NK1R-ir neurons (red) in contralateral preBötC. **B:** EGFP-expressing processes (green) from unilaterally injection into preBötC project to contralateral preBötC. **C:** Superimposition of (A) and (B); Some EGFP processes were found in juxtaposition to NK1R-ir neurons (red) in contralateral preBötC,. Blue box in outline represents area where images were acquired. Yellow arrows indicate NK1R-ir neurons. Magenta-green copy of this figure is available as Supporting Figure 4. Scale bar = 50 μm. [Color figure can be viewed in the online issue, which is available at www.interscience.wiley.com.]

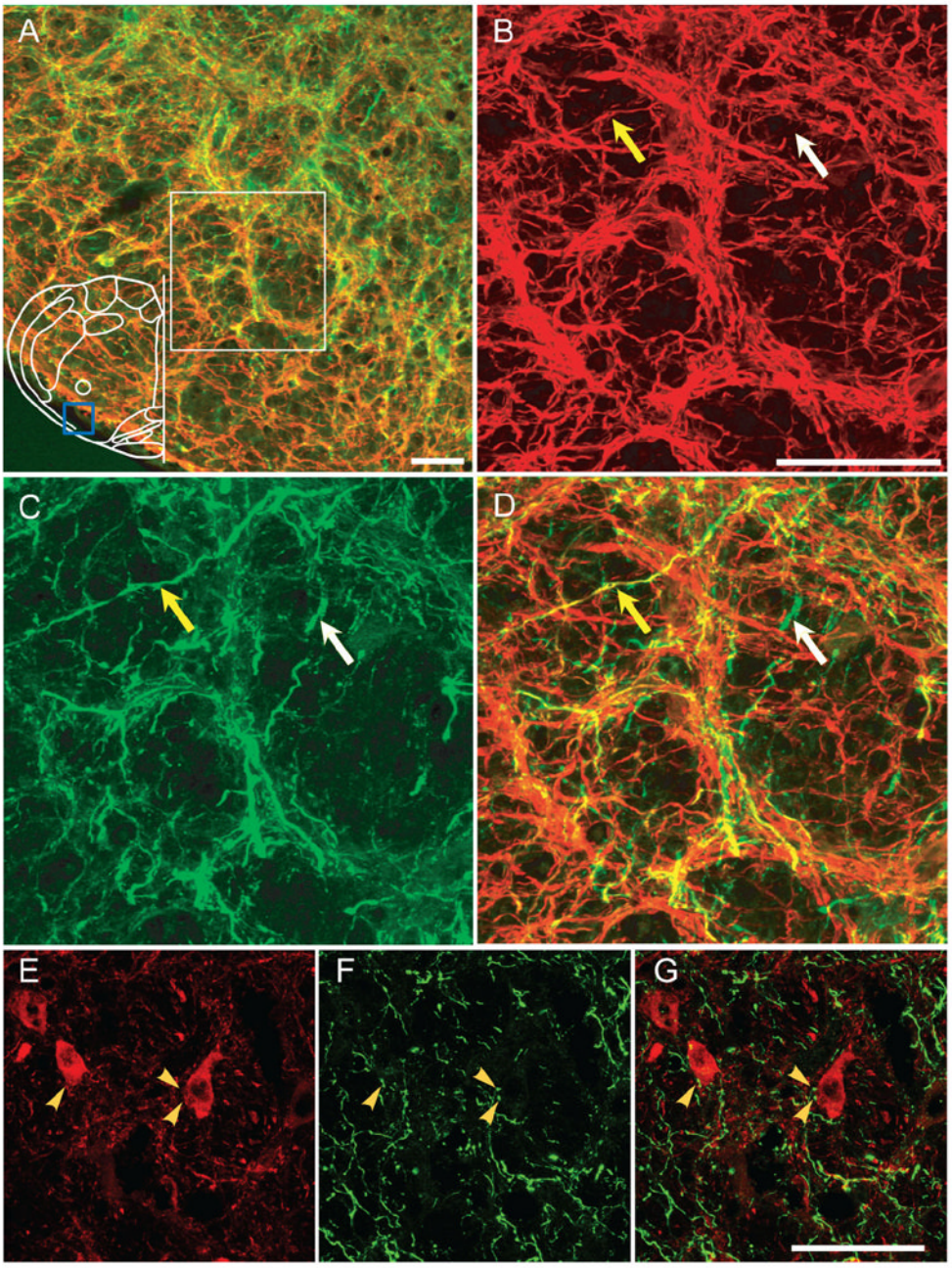

Figure 5. (Overleaf) PreBötC projections to ipsilateral BötC

A: EGFP-expressing processes from unilaterally injection into preBötC project to ipsilateral BötC. Few EGFP processes (green) were MAP2-ir (red) (mainly in the most caudal portion of BötC). Blue box in outline represents area where images were acquired. **B–D:** Higher magnification of immunoreactivity for MAP2 (B), EGFP (C), and overlap (D) from the region in white box of (A) in ipsilateral BötC. White arrow indicates absence of colocalization between EGFP and MAP2, whereas yellow arrow indicates colocalization. **E:** PV-ir neurons (red) in BötC. **F:** EGFP-expressing processes (green) from unilateral injection projecting into BötC. **G:** Superimposition of (E) and (F), showing some EGFP processes in juxtaposition to PV-ir neurons in BötC. Yellow arrows indicate occurrence of direct contacts of EGFP-expressing processes on to PV BötC neurons. Magenta-green copy of this figure is

available as Supporting Figure 5. Scale bars = 50 μm. [Color figure can be viewed in the online issue, which is available at www.interscience.wiley.com.]

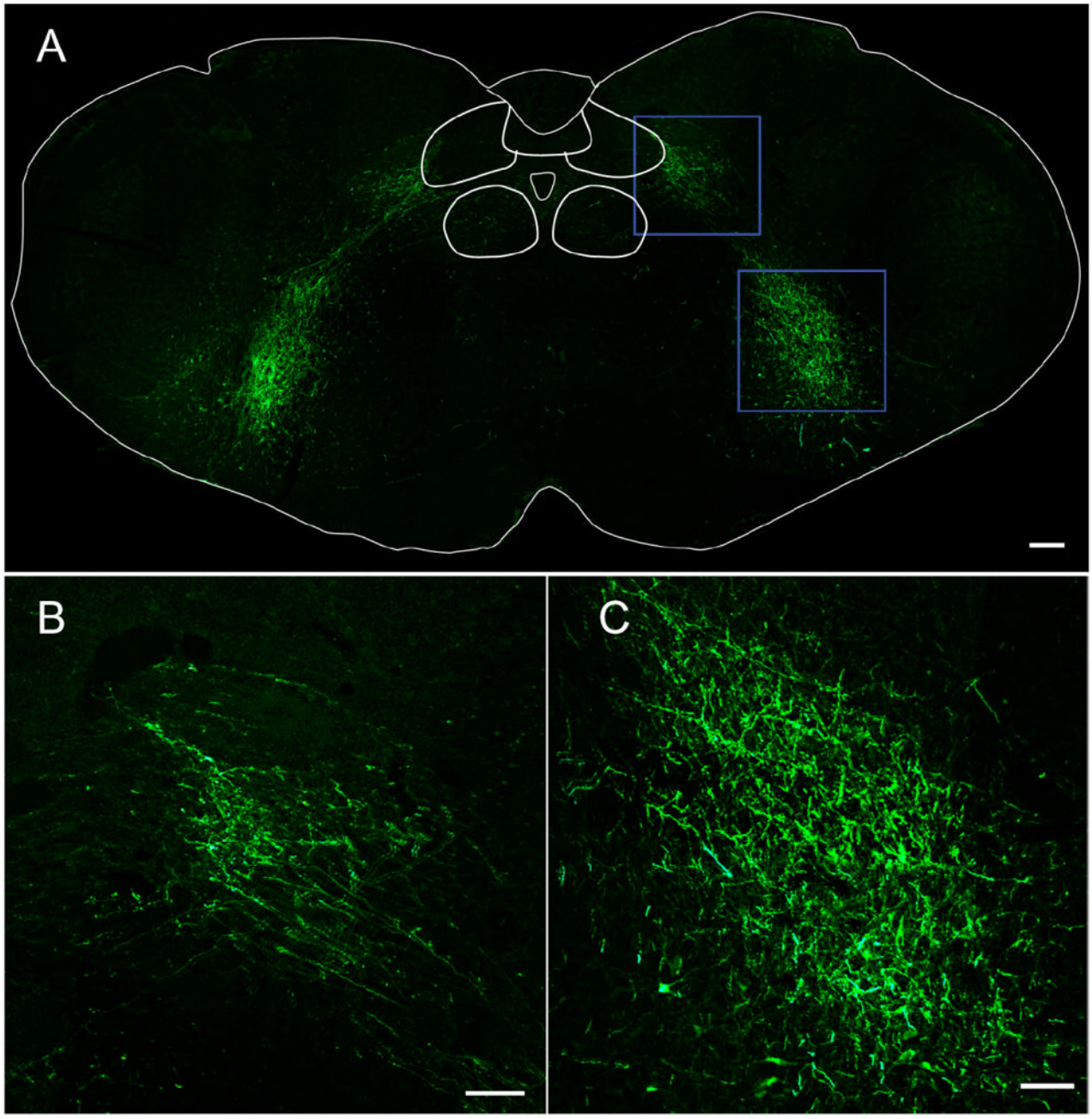

Figure 6. PreBötC neurons project to VRG and parahypoglossal/NTS region

A: Bilateral injection into preBötC revealed EGFP-expressing axons in parahypoglossal/NTS regions (top) and VRG caudal to preBötC (bottom). No EGFP-expressing cell bodies were observed. **B:** Parahypoglossal/NTS and **C:** VRG: higher magnification from these regions in top and bottom blue boxes of (A). Scale bars = 100 μm. [Color figure can be viewed in the online issue, which is available at www.interscience.wiley.com.]

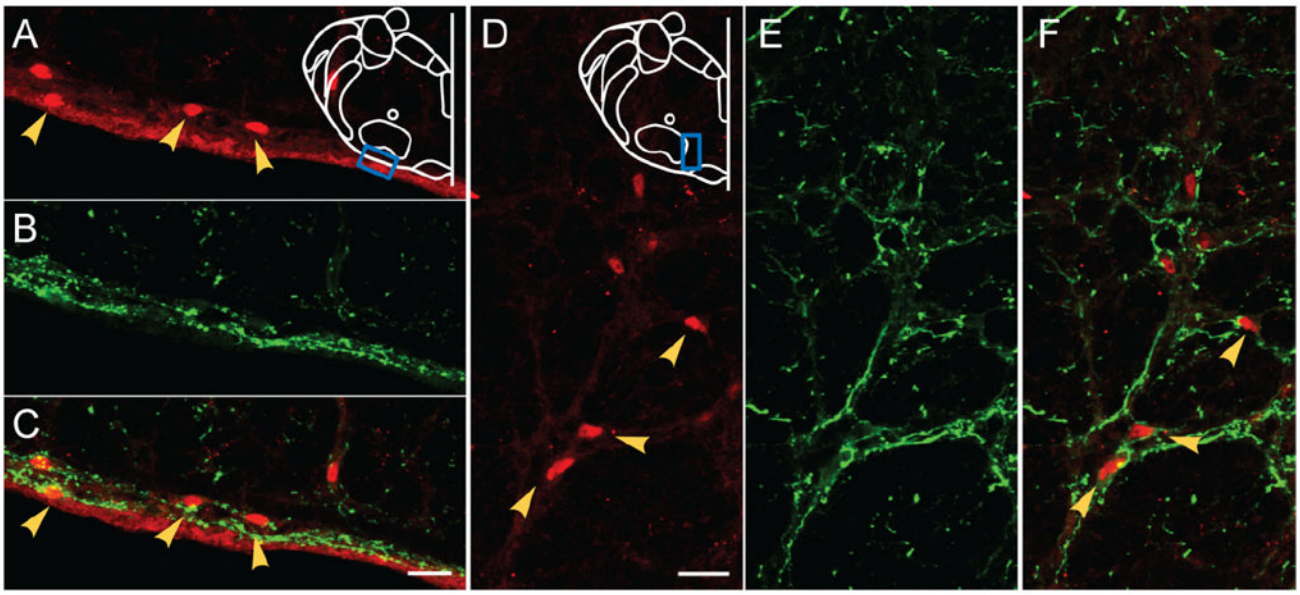

Figure 7. Projections to the pFRG/RTN region surrounding the facial nucleus

A,D: Phox2b-ir neurons (red) in ventral surface (A) and the region medial to the facial nucleus (D) in pFRG/RTN. **B,E:** EGFP-expressing processes (green) from unilateral injection into preBötC project to the ventral surface (B) and the region medial to facial nucleus (E) in pFRG/RTN. **C,F:** Superimposition of (A,B) and (D,E), respectively, showing some EGFP processes in juxtaposition to Phox2b-ir neurons in pFRG/RTN. Blue boxes in outlines represent areas where images were acquired. Yellow arrows indicate Phox2b-ir neurons. Magenta-green copy of this figure is available as Supporting Figure 6. Scale bars = 20 μm. [Color figure can be viewed in the online issue, which is available at www.interscience.wiley.com.]

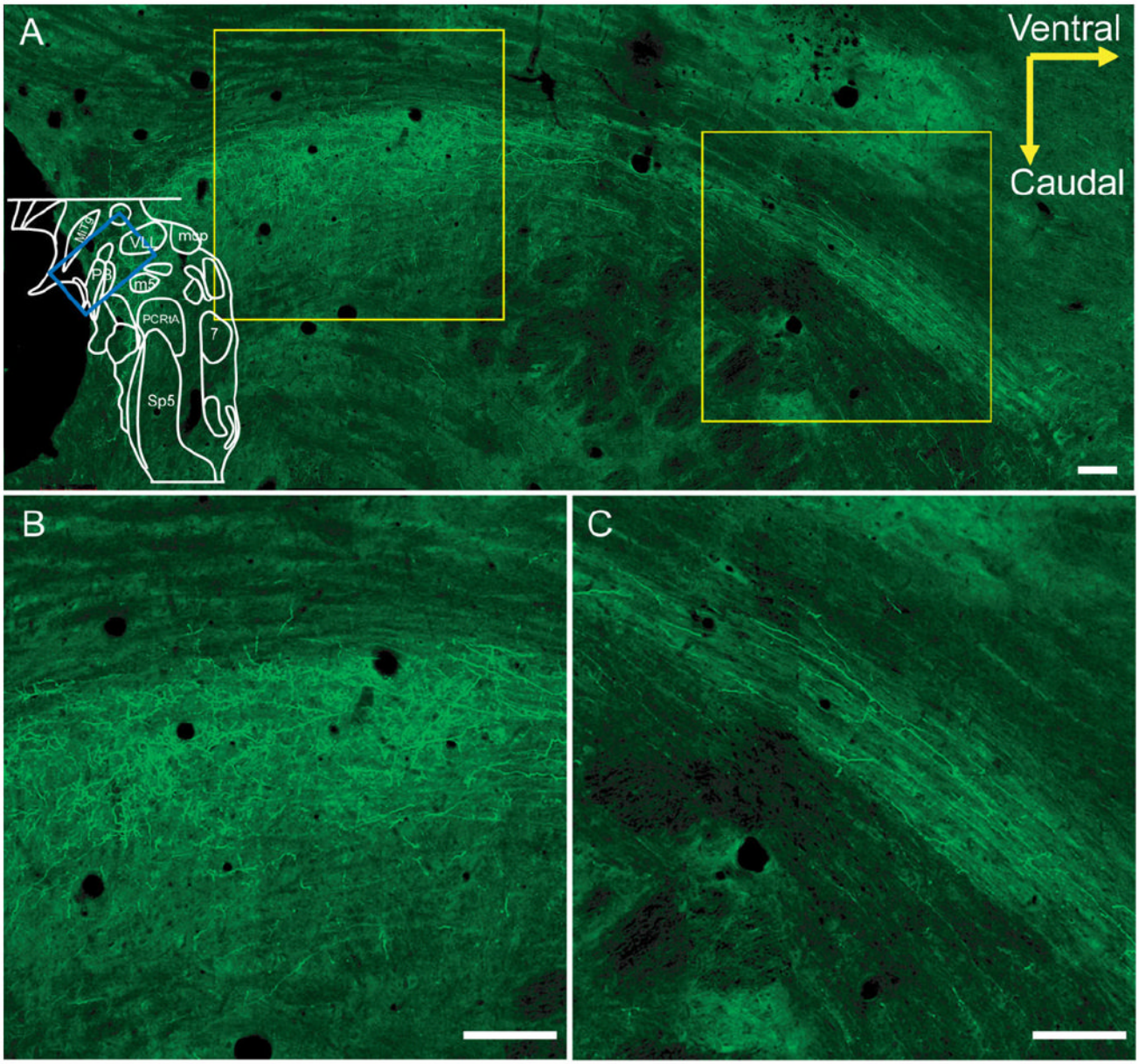

Figure 8. Projections to PB/KF

A: Sagittal view of EGFP-expressing axons in PB/KF following bilateral preBötC injection. Blue box in outline represents area where image was acquired. **B,C:** Higher-magnification view from regions in right and left white boxes of (A), respectively, demonstrating innervation of PB/KF (B) and bundle of axons directed to the area (C). Scale bars = 100 μm. [Color figure can be viewed in the online issue, which is available at www.interscience.wiley.com.]

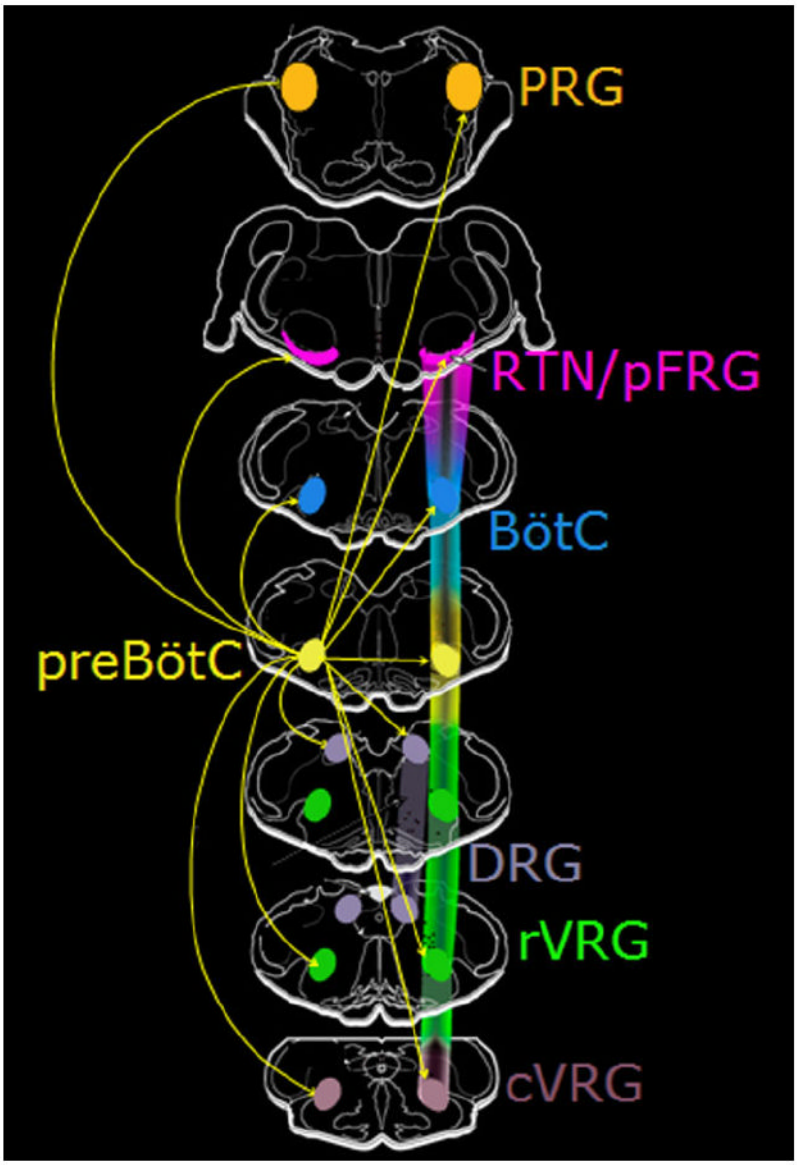

Figure 9. The projection network of preBötC complex neurons in brainstem

PreBötC complex neurons send brainstem projections to: contralateral preBötC, ipsi- and contralateral BötC, rVRG, dorsal respiratory group (DRG), RTN/pFRG, and pontine respiratory group (PRG). Magenta-green copy of this figure is available as Supporting Figure 7. [Color figure can be viewed in the online issue, which is available at www.interscience.wiley.com.]

TABLE 1

Primary Antibody Information

Antigen	Immunogen	Manufacturer/cat. no.	Dilution
NK1R	Synthetic peptide, aa 393-407 of NK1R	Advanced Targeting System, San Diego, CA; rabbit polyclonal, #AB-N04	1:1,000
Sst	Synthetic peptide, aa 1-14 from N-terminus of Sst protein	Peninsula Laboratories, Torrance, CA; rabbit polyclonal, #T-4103	1:500; or 1:5,000 for TSA
MAP2	Full-length protein (Cow)	Millipore, Billerica, MA; mouse monoclonal, SMI 52, #AB28032	1:1,000
EGFP	Purified recombinant EGFP	Aves Labs, Tigard, OR, chicken IgY, #GFP-1020	1:500
PV	Full-length protein of parvalbumin-19	Sigma, St. Louis, MO; mouse monoclonal, #P3088	1:2000
Phox2b	C-terminus 14 aa	Dr. JF Brunet, CNRS, Paris, France	1:800